Acta Mech Sin (2010) 26:881–888
DOI 10.1007/s10409-010-0384-x

RESEARCH PAPER

A strain-isolation design for stretchable electronics

Jian Wu · Ming Li · Wei-Qiu Chen · Dae-Hyeong Kim · Yun-Soung Kim · Yong-Gang Huang · Keh-Chih Hwang · Zhan Kang · John A. Rogers

Received: 2 August 2010 / Revised: 30 September 2010 / Accepted: 30 September 2010 / Published online: 2 December 2010
© The Chinese Society of Theoretical and Applied Mechanics and Springer-Verlag GmbH 2010

Abstract Stretchable electronics represents a direction of recent development in next-generation semiconductor devices. Such systems have the potential to offer the performance of conventional wafer-based technologies, but they can be stretched like a rubber band, twisted like a rope, bent over a pencil, and folded like a piece of paper. Isolating the active devices from strains associated with such deformations is an important aspect of design. One strategy involves the shielding of the electronics from deformation of the substrate through insertion of a compliant adhesive layer. This paper establishes a simple, analytical model and validates the results by the finite element method. The results show that a relatively thick, compliant adhesive is effective to reduce the strain in the electronics, as is a relatively short film.

Keywords Strain isolation · Thin film · Substrate · Adhesive · Stretchable electronics

The project was supported by NSF (DMI-0328162 and ECCS-0824129), the National Natural Science Foundation of China (10820101048), Ministry of Education of China, and the National Basic Research Program of China (2007CB936803).

J. Wu · M. Li · Y.-G. Huang (✉)
Departments of Civil and Environmental Engineering, and Mechanical Engineering, Northwestern University, Evanston, IL 60208, USA
e-mail: y-huang@northwestern.edu

M. Li · Z. Kang
Department of Engineering Mechanics, Dalian University of Technology, Dalian 116024, China

W.-Q. Chen
Department of Engineering Mechanics, Zhejiang University, Hangzhou 310058, China

D.-H. Kim · Y.-S. Kim · J. A. Rogers
Materials Research Laboratory, Department of Materials Science and Engineering, Beckman Institute, University of Illinois, Urbana, IL 61801, USA

K.-C. Hwang
AML, Department of Engineering Mechanics, Tsinghua University, Beijing 100084, China

J. A. Rogers
Departments of Chemistry, Electrical and Computer Engineering, and Mechanical Science and Engineering, University of Illinois, Urbana, IL 61801, USA

1 Introduction

The electronics industry has always pushed for the development of smaller and faster devices. These devices are confined to the planar surfaces of silicon wafers, and as a result, they are hard, rigid and flat. A new direction has recently emerged in the development of next-generation inorganic electronics, namely the stretchable electronics, that offer the performance of conventional wafer-based devices, but can be stretched like a rubber band, twisted like a rope, bent over a pencil, and folded like a piece of paper [1,2]. Stretchable electronics offers many new application opportunities, particularly for integration with tissues of human body to develop conformal, bio-interfaced electronics for cardiac electrophysiology [3] and electrocorticography [4], and electronic skin [5]. Other examples include cameras inspired by human eyes [6–8], stretchable, twistable, bendable and foldable circuits [9–12], flexible inorganic solar cells [13,14], and LEDs for deformable and semi-transparent displays [15,16]. See the review paper [2] on the recent progress and future directions of stretchable electronics.

Stretchable electronics is achieved by using elastomeric stamps to transfer print the conventional, inorganic electronics from their hard, rigid growth substrates (e.g., semiconductor wafers) to soft, elastic elastomeric substrates [17–24]. By controlling the peeling speed [20,23] or microstructures on the stamp surface [24], the stamp can pick up electronics from its growth substrate and print it on various receiver substrates, such as fabric, vinyl, leather, and paper [25].

Inorganic electronics transfer printed onto stretchable, elastomeric substrates, however, are not stretchable yet if the electronics remains flat (straight). This is because inorganic semiconductors fracture at ∼1% tensile strain. Several strategies discussed below, together with transfer printing, make inorganic electronics stretchable to 10% or even 100% strain.

(1) Pre-stretch of elastomeric substrates prior to transfer printing. Inorganic electronics is transferred printed onto a pre-stretched elastomeric substrate. Upon release of the pre-stretch, the thin electronics buckles on the surface of elastomer, and enables stretchability in the buckle direction [26]. This strategy has produced stretchable silicon ribbons [26–28], membranes [29,30] and nanowires [31–33], carbon nanotubes [34–36], and gold films [37]. Mechanics models have been developed to study various aspects of these systems, such as free edge [38], width [39], encapsulation [40], buckling modes [41,42], and elastic anisotropy [43–45] of the thin film; surface waviness [46,47], biaxial stretchability [48–52], finite deformation [53,54], and viscosity [55] of the substrate; and interface adhesion [56]. The review papers on experiments are in Ref. [57] and mechanics models are in Ref. [58].

(2) Non-coplanar mesh layout of island-bridge structures. The two-dimensional inorganic semiconductor islands interconnected by thin metal/elastomer bridges provide another strategy for stretchable electronics [11]. For curvilinear metal/elastomer bridges, the island-bridge structures are transfer printed onto an elastomeric substrate without the pre-stretch. The stretch imposed on the system after transfer printing causes the curvilinear bridges to buckle, i.e., the so-called lateral buckling [59], which shields the inorganic semiconductor islands from deformation. This strategy provides large stretchability, as demonstrated in conformal, bio-interfaced electronics [3,4], electronic-eye cameras [6–8,60,61], deformable circuits [9–12], and LED for deformable and semi-transparent displays [15,16]. The review paper is in Ref. [62].

(3) Stretchable interconnect. Another strategy to stretchable electronics is to use interconnect lines of metals that are close to liquid at room temperature [63–67]. Metal interconnects confined to plastic substrate have also been used [68–74] because the constraint from substrate makes the metals more stretchable. These stretchable interconnects provide the stretchability at the system level.

(4) Strain isolation via an adhesive layer. An adhesive layer between inorganic electronics and elastomeric substrates is introduced during transfer printing [25,75,76]. This layer serves as a strain-isolation element to shield the electronics from the large strains in the stretched elastomeric substrates. This approach has been demonstrated in experiments [25].

The purpose of this paper is to establish a mechanics model for the strain-isolation approach discussed above. An analytical solution is obtained for a three-layer system, consisting of inorganic film, adhesive and substrate. The maximum strain in the inorganic film given by the analytical model agrees very well with the finite element analysis. The verified analytical model is useful to the optimal design of strain-isolation layer for stretchable electronics.

2 A model for thin film/adhesive/substrate

Figure 1 shows a schematic diagram of a PDMS adhesive layer between a Si thin film and a plastic substrate. The film and adhesive are much thinner than the substrate, i.e., thickness $h_f \le h_a \ll h_s$ (Fig. 1). The substrate is much stiffer than the adhesive, but much more compliant than the film, i.e., Young's modulus $E_a \ll E_s \ll E_f$. An example is the PDMS adhesive ($E_a = 2.0\,\text{MPa}$), plastic substrate ($E_s = 2.0\,\text{GPa}$), and Si film ($E_f = 130\,\text{GPa}$).

The film and substrate are modeled as elastic beams. As shown in Fig. 2, the bending moment, shear force and axial force (per unit width in the out-of-plane direction) are denoted by M_i, Q_i and N_i (i = f for film or i = s for substrate). The interface normal and shear stresses are denoted by σ and τ, respectively (Fig. 2).

Equilibrium of force and moment requires [77,78]

$$\frac{dM_i}{dX} - Q_i + \frac{1}{2}\tau h_i = 0, \quad (1)$$

$$\frac{dQ_i}{dX} \mp \sigma = 0, \quad (2)$$

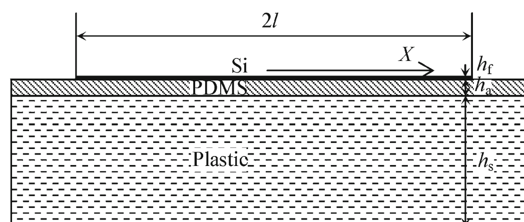

Fig. 1 Schematic diagram of a PDMS adhesive layer between a Si thin film and a plastic substrate

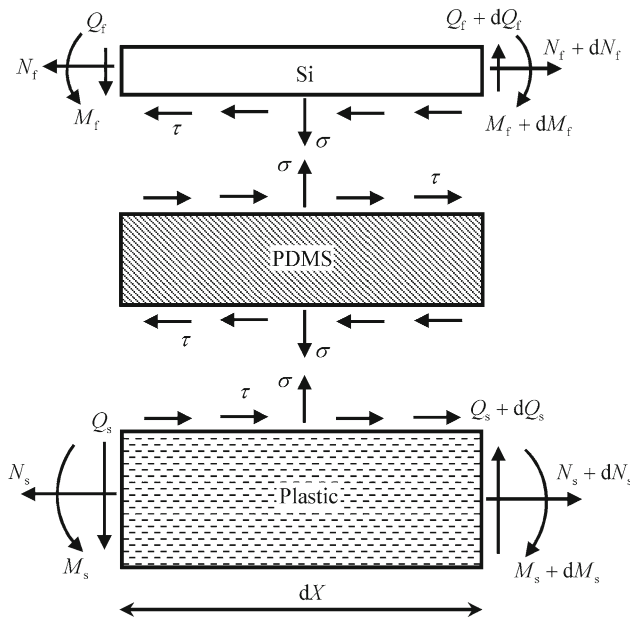

Fig. 2 Free-body diagram

$$\frac{dN_i}{dX} \mp \tau = 0, \tag{3}$$

where "−" in Eqs. (2) and (3) is for the film, and "+" is for the substrate. Elimination of the shear force from Eqs. (1) and (2) gives

$$\frac{d^2 M_i}{dX^2} \mp \sigma + \frac{h_i}{2}\frac{d\tau}{dX} = 0. \tag{4}$$

The axial force and bending moment are related to the axial and lateral displacements u_i and w_i in the film and substrate via the corresponding tension and bending rigidities,

$$\frac{du_i}{dX} = \frac{N_i}{\overline{E_i} h_i}, \tag{5}$$

$$\frac{d^2 w_i}{dX^2} = -\frac{12 M_i}{\overline{E_i} h_i^3}, \tag{6}$$

where $\overline{E_i} = E_i / \left(1 - \nu_i^2\right)$ is the plane-strain modulus.

The adhesive is thin and compliant, and therefore has negligible bending rigidity. Its constitutive model gives

$$\sigma = \overline{E_a} \frac{w_f - w_s}{h_a}, \tag{7}$$

$$\tau = G_a \frac{\left(u_f + \frac{h_f}{2}\frac{dw_f}{dX}\right) - \left(u_s - \frac{h_s}{2}\frac{dw_s}{dX}\right)}{h_a}, \tag{8}$$

where $\overline{E_a}$ and G_a are the plane-strain and shear moduli of the adhesive, and $u_f + (h_f/2)(dw_f/dX)$ and $u_s - (h_s/2)(dw_s/dX)$ are the axial displacements at the film/adhesive and adhesive/substrate interfaces, respectively.

Equations (2)–(8) give 12 equations for 12 variables, namely N_f, M_f, Q_f, u_f and w_f for the film, N_s, M_s, Q_s, u_s and w_s for the substrate, and σ and τ related to the adhesive. The traction-free boundary conditions at the ends of the thin film are

$$N_f = 0, \quad M_f = 0, \quad Q_f = 0, \quad \text{at} \quad X = \pm l, \tag{9}$$

where $2l$ is the film length, and $X = 0$ denotes the center of the film. The boundary conditions in the substrate are

$$N_s = 0, \quad M_s = M_0, \quad Q_s = 0, \quad \text{at} \quad X = \pm l, \tag{10}$$

where M_0 is the bending moment applied to the substrate. Equations (9) and (10), together with the conditions to eliminate rigid body motion, give all boundary conditions for Eqs. (2)–(8).

Elimination of axial forces, bending moments and displacements by substituting Eqs. (3)–(6) into the 4th order derivative of Eq. (7) and 3rd order derivative of Eq. (8) gives

$$\frac{h_a}{\overline{E_a}}\frac{d^4\sigma}{dX^4} + 12\left(\frac{1}{\overline{E_f} h_f^3} + \frac{1}{\overline{E_s} h_s^3}\right)\sigma - 6\left(\frac{1}{\overline{E_f} h_f^2} - \frac{1}{\overline{E_s} h_s^2}\right)\frac{d\tau}{dX} = 0, \tag{11}$$

$$\frac{h_a}{G_a}\frac{d^3\tau}{dX^3} - 4\left(\frac{1}{\overline{E_f} h_f} + \frac{1}{\overline{E_s} h_s}\right)\frac{d\tau}{dX} + 6\left(\frac{1}{\overline{E_f} h_f^2} - \frac{1}{\overline{E_s} h_s^2}\right)\sigma = 0. \tag{12}$$

Elimination of σ from the above two equations yields the following equation for τ

$$\frac{d^7\tau}{dX^7} - 4\frac{G_a}{h_a}\left(\frac{1}{\overline{E_f} h_f} + \frac{1}{\overline{E_s} h_s}\right)\frac{d^5\tau}{dX^5} + 12\frac{\overline{E_a}}{h_a}\left(\frac{1}{\overline{E_f} h_f^3} + \frac{1}{\overline{E_s} h_s^3}\right)\frac{d^3\tau}{dX^3} - 12\frac{\overline{E_a} G_a}{h_a^2} \times \left[4\frac{(h_f + h_s)^2}{\overline{E_f} h_f^3 \overline{E_s} h_s^3} + \left(\frac{1}{\overline{E_f} h_f^2} - \frac{1}{\overline{E_s} h_s^2}\right)^2\right]\frac{d\tau}{dX} = 0. \tag{13}$$

The following 3 conditions are useful in the next section for the limit of extremely compliant adhesive. The substitution of Eqs. (5) and (6) into the 1st order derivative of Eq. (8), together with boundary conditions (9) and (10), give

$$\left.\frac{d\tau}{dX}\right|_{X=\pm l} = -\frac{6 G_a}{h_a \overline{E_s} h_s^2} M_0. \tag{14}$$

The substitution of Eq. (6) into the 2nd order derivative of Eq. (7), together with boundary conditions (9) and (10), give

$$\left.\frac{d^2\sigma}{dX^2}\right|_{X=\pm l} = 12\frac{\overline{E_a}}{h_a \overline{E_s} h_s^3} M_0. \tag{15}$$

The integration of Eq. (2), together with the traction-free shear force in Eq. (9) (or Eq. (10)), gives

$$\int_{-l}^{l} \sigma \, \mathrm{d}X = 0. \tag{16}$$

3 Extremely compliant adhesive

A simple, analytical solution is obtained in this section for an extremely compliant adhesive with Young's modulus (e.g., 2.0 MPa for PDMS) several orders of magnitude smaller than the film (e.g, $E_f = 130$ GPa for Si) and substrate (e.g., $E_s = 2.0$ GPa for plastic). Here the film is sufficiently thin such that its tensile stiffness is less than, or on the same order as, the tensile stiffness of the substrate,

$$E_f h_f \le E_s h_s, \quad \text{or} \quad E_f h_f \sim E_s h_s. \tag{17}$$

For a 0.3 µm thick Si film [25], this requires the thickness of plastic substrate $h_s \ge 20$ µm. Since the film is much thinner than the substrate, Eq. (17) also indicates $E_f h_f^2 \ll E_s h_s^2$ and $E_f h_f^3 \ll E_s h_s^3$. Equation (13) is then simplified to

$$\frac{\mathrm{d}^7\tau}{\mathrm{d}X^7} - 4\frac{G_a}{h_a}\left(\frac{1}{\overline{E}_f h_f} + \frac{1}{\overline{E}_s h_s}\right)\frac{\mathrm{d}^5\tau}{\mathrm{d}X^5} + 12\frac{\overline{E}_a}{h_a \overline{E}_f h_f^3}\frac{\mathrm{d}^3\tau}{\mathrm{d}X^3} - 12\frac{\overline{E}_a G_a}{h_a^2 \overline{E}_f h_f^3}\left(\frac{1}{\overline{E}_f h_f} + \frac{4}{\overline{E}_s h_s}\right)\frac{\mathrm{d}\tau}{\mathrm{d}X} = 0. \tag{18}$$

Introduce a non-dimensional distance $\xi = \lambda X$, where

$$\lambda = \sqrt{\frac{G_a}{h_a}\left(\frac{1}{\overline{E}_f h_f} + \frac{4}{\overline{E}_s h_s}\right)}. \tag{19}$$

Equation (18) then becomes

$$\frac{1}{12}\frac{\overline{E}_a h_f}{\overline{E}_f h_a}\left(\frac{G_a}{\overline{E}_a}\right)^2\left(1 + \frac{4\overline{E}_f h_f}{\overline{E}_s h_s}\right)^2 \times \left(\frac{\mathrm{d}^7\tau}{\mathrm{d}\xi^7} - \frac{\overline{E}_f h_f + \overline{E}_s h_s}{\overline{E}_f h_f + \frac{\overline{E}_s h_s}{4}}\frac{\mathrm{d}^5\tau}{\mathrm{d}\xi^5}\right) + \frac{\mathrm{d}^3\tau}{\mathrm{d}\xi^3} - \frac{\mathrm{d}\tau}{\mathrm{d}\xi} = 0. \tag{20}$$

Its coefficient of the first term is very small because $\overline{E}_a / \overline{E}_f \ll 1$, $h_f / h_a \le 1$, $\left(G_a / \overline{E}_a\right)^2 \sim 1$, and $\left(1 + 4\left(\overline{E}_f h_f\right) / \left(\overline{E}_s h_s\right)\right)^2 \sim 1$. Therefore, the above equation is simplified to $\mathrm{d}^3\tau / \mathrm{d}\xi^3 - \mathrm{d}\tau / \mathrm{d}\xi = 0$, which has solution $\tau = A \sinh \xi$ due to asymmetry of the shear stress around the center $X = 0$, where the coefficient A is to be determined from the boundary condition (14). The shear stress is then obtained as

$$\tau = -\frac{6G_a}{\lambda h_a \overline{E}_s h_s^2} M_0 \frac{\sinh(\lambda X)}{\cosh(\lambda l)}, \tag{21}$$

which reaches the maximum shear stress at the end

$$\tau_{\max} = \frac{6G_a}{\lambda h_a \overline{E}_s h_s^2}\tanh(\lambda l) M_0. \tag{22}$$

Substitution of the shear stress above into Eq. (11) gives

$$\frac{h_a}{\overline{E}_a}\frac{\mathrm{d}^4\sigma}{\mathrm{d}X^4} + \frac{12}{\overline{E}_f h_f^3}\sigma = -\frac{36 G_a}{h_a \overline{E}_f h_f^2 \overline{E}_s h_s^2} M_0 \frac{\cosh(\lambda X)}{\cosh(\lambda l)}, \tag{23}$$

under the condition (17). Its solution is symmetric about $X = 0$, and is given by

$$\sigma = -\frac{3G_a h_f}{h_a \overline{E}_s h_s^2} M_0 \frac{\cosh(\lambda X)}{\cosh(\lambda l)} + B \sinh(\kappa X)\sin(\kappa X) + C\cosh(\kappa X)\cos(\kappa X), \tag{24}$$

under the condition (17), $\overline{E}_a / \overline{E}_f \ll 1$ and $h_f / h_a \le 1$, where B and C are the coefficients to be determined, and

$$\kappa = \left(\frac{3\overline{E}_a}{h_a \overline{E}_f h_f^3}\right)^{1/4}. \tag{25}$$

The boundary conditions (15) and (16) become

$$B\cosh(\kappa l)\cos(\kappa l) - C\sinh(\kappa l)\sin(\kappa l) = \frac{2}{\overline{E}_s h_s^3}\sqrt{\frac{3\overline{E}_a \overline{E}_f h_f^3}{h_a}} M_0, \tag{26}$$

$$(B + C)\cosh(\kappa l)\sin(\kappa l) - (B - C)\sinh(\kappa l)\cos(\kappa l) = \frac{6\kappa G_a h_f}{\lambda h_a \overline{E}_s h_s^2}\tanh(\lambda l) M_0, \tag{27}$$

which have the solution

$$B = \left\{3\frac{\kappa G_a h_f h_s}{\lambda h_a}\tanh(\lambda l) + \sqrt{\frac{3\overline{E}_a \overline{E}_f h_f^3}{h_a}}\left[\coth(\kappa l) + \cot(\kappa l)\right]\right\} \times \frac{4}{\overline{E}_s h_s^3}\frac{\sinh(\kappa l)\sin(\kappa l)}{\sinh(2\kappa l) + \sin(2\kappa l)} M_0, \tag{28}$$

$$C = \left\{3\frac{\kappa G_a h_f h_s}{\lambda h_a}\tanh(\lambda l) + \sqrt{\frac{3\overline{E}_a \overline{E}_f h_f^3}{h_a}}\left[\tanh(\kappa l) - \tan(\kappa l)\right]\right\} \times \frac{4}{\overline{E}_s h_s^3}\frac{\cosh(\kappa l)\cos(\kappa l)}{\sinh(2\kappa l) + \sin(2\kappa l)} M_0, \tag{29}$$

under the condition (17), $\overline{E}_a / \overline{E}_f \ll 1$ and $h_f / h_a \le 1$.

The membrane strain in the film is obtained from Eqs. (3) and (5), and boundary condition (9) as

$$\frac{du_f}{dX} = \frac{N_f}{\overline{E}_f h_f} = \frac{-1}{\overline{E}_f h_f}\int_X^l \tau \, dX = \frac{6}{\left(1+\frac{4\overline{E}_f h_f}{\overline{E}_s h_s}\right)\overline{E}_s h_s^2} M_0 \left[1 - \frac{\cosh(\lambda X)}{\cosh(\lambda l)}\right], \quad (30)$$

which reaches the maximum $\left\{1\big/\left[1+(4\overline{E}_f h_f)\big/(\overline{E}_s h_s)\right]\right\}\left\{1-1\big/[\cosh(\lambda l)]\right\}(6M_0)\big/\left(\overline{E}_s h_s^2\right)$ at the center $X = 0$.

The shear force in the film is obtained from Eq. (2) and the anti-symmetry condition $Q_f\,|_{X=0} = 0$ as

$$Q_f = \int_0^X \sigma \, dX = -\frac{3G_a h_f}{\lambda h_a \overline{E}_s h_s^2} M_0 \frac{\sinh(\lambda X)}{\cosh(\lambda l)} + \frac{B+C}{2\kappa}\cosh(\kappa X)\sin(\kappa X) - \frac{B-C}{2\kappa}\sinh(\kappa X)\cos(\kappa X). \quad (31)$$

The bending moment is then obtained from Eq. (1) and the boundary condition (9) as

$$M_f = -\int_X^l \left(Q_f - \frac{1}{2}\tau h_f\right) dX = \frac{\overline{E}_f h_f^3}{\overline{E}_s h_s^3} M_0 - \frac{B}{2\kappa^2}\cosh(\kappa X)\cos(\kappa X) + \frac{C}{2\kappa^2}\sinh(\kappa X)\sin(\kappa X), \quad (32)$$

which also reaches the maximum $\left(\overline{E}_f h_f^3\right)\big/\left(\overline{E}_s h_s^3\right) M_0 - \left(B\big/2\kappa^2\right)$ at the center $X = 0$. The maximum bending strain in the film $(6M_f)\big/(\overline{E}_f h_f^2)$ reaches maximum $(6h_f M_0)\big/(\overline{E}_s h_s^3) - 3B\big/\left(\kappa^2 \overline{E}_f h_f^2\right)$ at the center $X = 0$.

The maximum strain in the film is the sum of the corresponding membrane and bending strains at the center, and is given by

$$(\varepsilon_f)_{max} = \left[\frac{1-\frac{1}{\cosh(\lambda l)}}{1+\frac{4\overline{E}_f h_f}{\overline{E}_s h_s}} + \frac{h_f}{h_s}\right]\frac{6M_0}{\overline{E}_s h_s^2} - \frac{3B}{\kappa^2 \overline{E}_f h_f^2}. \quad (33)$$

For a vanishing adhesive layer $h_a \to 0$, the above maximum strain degenerates to

$$(\varepsilon_f)_{\text{no adhesive}} = \frac{6M_0}{\overline{E}_s h_s^2}\Bigg/\left(1+\frac{4\overline{E}_f h_f}{\overline{E}_s h_s}\right), \quad (34)$$

which is the maximum strain in a composite beam of thin film and substrate (no adhesive) under the condition $h_f \ll h_s$.

The ratio of the maximum strain in Eq. (33) to its counterpart without the adhesive in Eq. (34), $(\varepsilon_f)_{max}\big/(\varepsilon_f)_{\text{no adhesive}}$, reflects the strain reduction in the film due to the adhesive, and is presented in the following. Unless otherwise specified, the thickness and elastic properties are $h_a = 10\,\mu$m, $E_a = 2.0$ MPa and Poisson's ratio $\nu_a = 0.48$ for the PDMS adhesive, $h_s = 100\,\mu$m, $E_s = 2.0$ GPa and $\nu_s = 0.34$ for the plastic substrate, and $h_f = 0.3\,\mu$m, $E_f = 130$ GPa, $\nu_f = 0.27$, and length $2l = 300\,\mu$m for the Si film [25].

Figure 3 clearly shows that the strain ratio $(\varepsilon_f)_{max}\big/(\varepsilon_f)_{\text{no adhesive}}$ decreases rapidly as the thickness h_a of the adhesive increases. A $1\,\mu$m-thick adhesive reduces the film strain by a factor of 4, and a $10\,\mu$m-thick adhesive reduces it 28 times. This is because a very compliant adhesive isolates the film from substrate bending, and a thicker adhesive is more effective in this strain isolation. The finite element method is also used to determine the strain ratio in the film, with and without the adhesive. The numerical results, also shown in Fig. 3, agree very well with the analytical solution, and therefore validate the present model.

Figure 4 shows that the strain ratio $(\varepsilon_f)_{max}\big/(\varepsilon_f)_{\text{no adhesive}}$ increases with the Young's modulus of adhesive. For the adhesive Young's modulus 0.1, 2 and 10 MPa, the film strain is reduced by ~150, 28 and 7 times, respectively. As the compliance of the adhesive increases, the film is shielded more effectively from the substrate deformation.

The strain isolation is also more effective for a short film than a long one, as shown in Fig. 5. The strain ratio is 0.036 for a $300\,\mu$m-long film, and increases to 0.12 for a $600\,\mu$m-long film, which correspond to strain reduction of 28 and 8 times, respectively. Except for very short films, the bending strain is negligible as compared with the membrane strain, and the latter can be written as $[1-1/\cosh(\lambda l)](\varepsilon_f)_{\text{no adhesive}}$, which decreases rapidly with the film length.

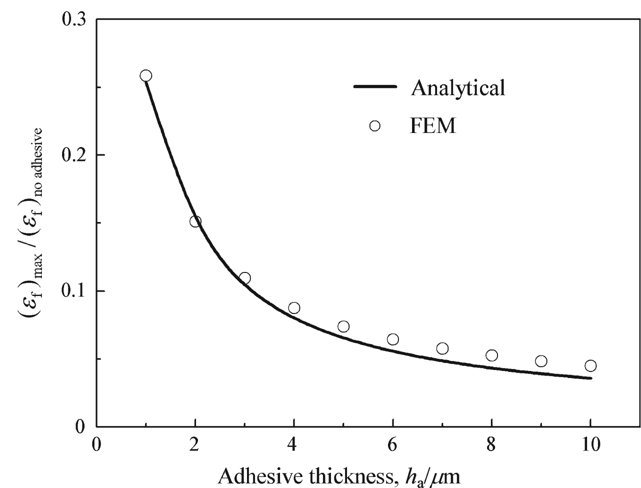

Fig. 3 The ratio of film strains with and without the adhesive, $(\varepsilon_f)_{max}\big/(\varepsilon_f)_{\text{no adhesive}}$, versus the adhesive thickness h_a. Results are shown for both the analytical model and the finite element method

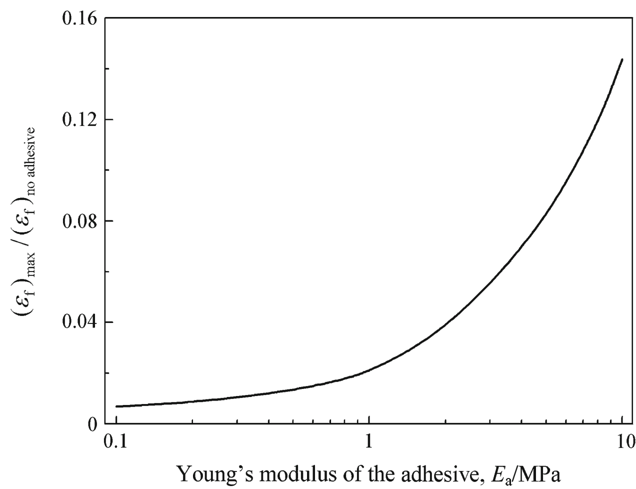

Fig. 4 The ratio of film strains with and without the adhesive, $(\varepsilon_f)_{max} / (\varepsilon_f)_{no\ adhesive}$, versus the Young's modulus of the adhesive E_a

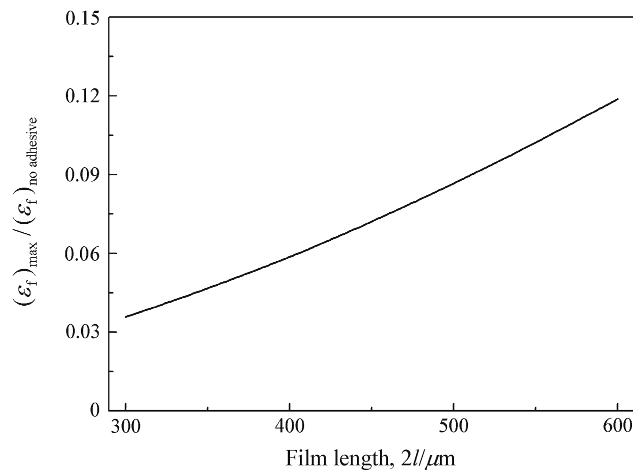

Fig. 5 The ratio of film strains with and without the adhesive, $(\varepsilon_f)_{max} / (\varepsilon_f)_{no\ adhesive}$, versus the film length $2l$

4 Conclusions

A simple, analytical model is established for the strain isolation approach to stretchable electronics. A compliant adhesive between an inorganic film and a plastic substrate shields the film from substrate deformation. The simple, analytical solution is validated by the finite element method, and is useful to the optimal design for stretchable electronics. The analytical model shows that a relatively thick, compliant adhesive is effective to reduce the film strain, and so is a relatively short film.

References

1. Rogers, J.A., Huang, Y.: A curvy, stretchy future for electronics. PNAS **106**, 10875–10876 (2009)
2. Rogers, J.A., Someya, T., Huang, Y.: Materials and mechanics for stretchable electronics. Science **327**, 1603–1607 (2010)
3. Viventi, J., Kim, D.H., Moss, J.D., et al.: A conformal, bio-interfaced class of silicon electronics for mapping cardiac electrophysiology. Sci. Transl. Med. **2**, 24ra22 (2010)
4. Kim, D.H., Viventi, J., Amsden, J.J., et al.: Dissolvable films of silk fibroin for ultrathin, conformal bio-integrated electronics. Nat. Mater. **9**, 511–517 (2010)
5. Wagner, S., Lacour, S.P., Jones, J., et al.: Electronic skin: architecture and components. Physica E **25**, 326–334 (2005)
6. Ko, H.C., Stoykovich, M.P., Song, J., et al. : A hemispherical electronic eye camera based on compressible silicon optoelectronics. Nature **454**, 748–753 (2008)
7. Ko, H.C., Shin, G., Wang, S., et al. : Curvilinear electronics formed using silicon membrane circuits and elastomeric transfer elements. Small **5**, 2703–2709 (2009)
8. Shin, G., Jung, I., Malyarchuk, V., et al. : Micromechanics and advanced designs for curved photodetector arrays in hemispherical electronic eye cameras. Small **6**, 851–856 (2010)
9. Kim, D.H., Ahn, J.H, Choi, W.M., et al.: Stretchable and foldable silicon integrated circuits. Science **320**, 507–511 (2008)
10. Kim, D.H., Choi, W.M., Ahn, J.H., et al.: Complementary metal oxide silicon integrated circuits incorporating monolithically integrated stretchable wavy interconnects. Appl. Phys. Lett. **93**, 044102 (2008)
11. Kim, D.H., Song, J., Choi, W.M., et al. : Materials and noncoplanar mesh designs for integrated circuits with linear elastic responses to extreme mechanical deformations. PNAS **105**, 18675–18680 (2008)
12. Kim, D.H., Liu, Z., Kim, Y.S., et al. : Optimized structural designs for stretchable silicon integrated circuits. Small **5**, 2841–2847 (2009)
13. Yoon, J., Baca, A.J., Park, S.I., et al.: Ultrathin silicon solar microcells for semitransparent, mechanically flexible and microconcentrator module designs. Nat. Mater. **7**, 907–915 (2008)
14. Baca, A.J., Yu, K.J., Xiao, J., et al.: Compact monocrystalline silicon solar modules with high voltage outputs and mechanically flexible designs. Energy Environ. Sci. **3**, 208–211 (2010)
15. Park, S.L., Xiong, Y., Kim, R.H., et al. : Printed assemblies of inorganic light-emitting diodes for deformable and semitransparent displays. Science **325**, 977–981 (2009)
16. Park, S.I., Le, A.P., Wu, J., et al.: Light emission characteristics and mechanics of foldable inorganic light-emitting diodes. Adv. Mater. **22**, 3062–3066 (2010)
17. Huang, Y., Zhou, W., Hsia, K.J., et al. : Stamp collapse in soft lithography. Langmuir **21**, 8058–8068 (2005)
18. Hsia, K.J., Huang, Y., Menard, E., et al. : Collapse of stamps for soft lithography due to interfacial adhesion. Appl. Phys. Lett. **86**, 154106 (2005)
19. Zhou, W., Huang, Y., Menard, E., et al. : Mechanism for stamp collapse in soft lithography. Appl. Phys. Lett. **87**, 251925 (2005)
20. Meitl, M.A., Zhu, Z.T., Kumar, V., et al. : Transfer printing by kinetic control of adhesion to an elastomeric stamp. Nat. Mater. **5**, 33–38 (2006)
21. Meitl, M.A., Feng, X., Dong, J., et al. : Stress focusing for controlled fracture in microelectromechanical systems. Appl. Phys. Lett. **90**, 083110 (2007)
22. Feng, X., Meitl, M.A., Bowen, A.M., et al. : Competing fracture in kinetically controlled transfer printing. Langmuir **23**, 12555–12560 (2007)
23. Kim, T.H., Carlson, A., Ahn, J.H., et al. : Kinetically controlled, adhesiveless transfer printing using microstructured stamps. Appl. Phys. Lett. **94**, 113502 (2009)
24. Kim, S., Wu, J., Carlson, A., et al.: Microstructured elastomeric surfaces with reversible adhesion and examples of their use in deterministic assembly by transfer printing. PNAS. **107**, 17095–17100 (2010)

25. Kim, D.H., Kim, Y.S., Wu, J., et al.: Ultrathin silicon circuits with strain-isolation layers and mesh layouts for high-performance electronics on fabric, vinyl, leather, and paper. Adv. Mater. **21**, 3703–3707 (2009)
26. Khang, D.Y., Jiang, H., Huang, Y., et al.: A stretchable form of single-crystal silicon for high-performance electronics on rubber substrates. Science **311**, 208–212 (2006)
27. Sun, Y., Choi, W.M., Jiang, H., et al.: Controlled buckling of semiconductor nanoribbons for stretchable electronics. Nat. Nanotechnol. **1**, 201–207 (2006)
28. Jiang, H., Sun, Y., Rogers, J.A., et al.: Mechanics of precisely controlled thin film buckling on elastomeric substrate. Appl. Phys. Lett. **90**, 133119 (2007)
29. Choi, W.M., Song, J., Khang, D.Y., et al.: Biaxially stretchable "Wavy" silicon nanomembranes. Nano Lett. **7**, 1655–1663 (2007)
30. Song, J., Jiang, H., Choi, W.M., et al.: An analytical study of two-dimensional buckling of thin films on compliant substrates. J. Appl. Phys. **103**, 014303 (2008)
31. Ryu, S.Y., Xiao, J., Park, W., et al.: Lateral buckling mechanics in silicon nanowires on elastomeric substrates. Nano Lett. **9**, 3214–3219 (2009)
32. Xiao, J., Ryu, S.Y., Huang, Y., et al.: Mechanics of nanowire/nanotube in-surface buckling on elastomeric substrates. Nanotechnology **21**, 085708 (2010)
33. Song, T., Xia, J., Lee, J.H., et al.: Arrays of sealed silicon nanotubes as anodes for lithium ion batteries. Nano Lett. **10**, 1710–1716 (2010)
34. Khang, D.Y., Xiao, J., Kocabas, C., et al.: Molecular scale buckling mechanics on individual aligned single-wall carbon nanotubes on elastomeric substrates. Nano Lett. **8**, 124–130 (2008)
35. Xiao, J., Jiang, H., Khang, D.Y., et al.: Mechanics of buckled carbon nanotubes on elastomeric substrates. J. Appl. Phys. **104**, 033543 (2008)
36. Xiao, J., Dunham, S., Liu, P., et al.: Alignment controlled growth of single-walled carbon nanotubes on quartz substrates. Nano Lett. **9**, 4311–4319 (2009)
37. Bowden, N., Brittain, S., Evans, A.G., et al.: Spontaneous formation of ordered structures in thin films of metals supported on an elastomeric polymer. Nature **393**, 146–149 (1998)
38. Koh, C.T., Liu, Z.J., Khang, D.Y., et al.: Edge effects in buckled thin films on elastomeric substrates. Appl. Phys. Lett. **91**, 133113 (2007)
39. Jiang, H., Khang, D.Y., Fei, H., et al.: Finite width effect of thin-films buckling on compliant substrate: experimental and theoretical studies. J. Mech. Phys. Solids **56**, 2585–2598 (2008)
40. Jiang, H., Sun, Y., Rogers, J.A., et al.: Post-buckling analysis for the precisely controlled buckling of thin film encapsulated by elastomeric substrates. Int. J. Solids Struct. **45**, 2014–2023 (2008)
41. Mei, H., Chung, J.Y., Yu, H.H., et al.: Buckling modes of elastic thin films on elastic substrates. Appl. Phys. Lett. **90**, 151902 (2007)
42. Wang, S., Song, J., Kim, D.H., et al.: Local versus global buckling of thin films on elastomeric substrates. Appl. Phys. Lett. **93**, 023126 (2008)
43. Im, S.H., Huang, R.: Wrinkle patterns of anisotropic crystal films on viscoelastic substrates. J. Mech. Phys. Solids **56**, 3315–3330 (2008)
44. Pang, Y., Huang, R.: Effect of elastic anisotropy on surface pattern evolution of epitaxial thin films. Int. J. Solids Struct. **46**, 2822–2833 (2009)
45. Song, J.: Herringbone buckling patterns of anisotropic thin films on elastomeric substrates. Appl. Phys. Lett. **96**, 051913 (2010)
46. Xiao, J., Carlson, A., Liu, Z.J., et al.: Stretchable and compressible thin films of stiff materials on compliant wavy substrates. Appl. Phys. Lett. **93**, 013109 (2008)
47. Xiao, J., Carlson, A., Liu, Z., et al.: Analytical and experimental studies of the mechanics of deformation in a solid with a wavy surface profile. J. Appl. Mech. **77**, 011003 (2010)
48. Chen, X., Hutchinson, J.W.: Herringbone buckling patterns of compressed thin films on compliant substrates. J. Appl. Mech. **71**, 597–603 (2004)
49. Huang, Z.Y., Hong, W., Suo, Z.: Nonlinear analyses of wrinkles in a film bonded to a compliant substrate. J. Mech. Phys. Solids **53**, 2101–2118 (2005)
50. Audoly, B., Boudaoud, A.: Buckling of a stiff film bound to a compliant substrate—Part I: Formation, linear stability of cylindrical patters, secondary bifurcations. J. Mech. Phys. Solids **56**, 2401–2421 (2008)
51. Audoly, B., Boudaoud, A.: Buckling of a stiff film bound to a compliant substrate—Part II: A global scenario for the formation of herringbone pattern. J. Mech. Phys. Solids **56**, 2422–2443 (2008)
52. Audoly, B., Boudaoud, A.: Buckling of a stiff film bound to a compliant substrate—Part III: Herringbone solutions at large buckling parameter. J. Mech. Phys. Solids **56**, 2444–2458 (2008)
53. Jiang, H., Khang, D.Y., Song, J., et al.: Finite deformation mechanics in buckled thin films on compliant supports. PNAS **104**, 15607–15612 (2007)
54. Song, J., Jiang, H., Liu, Z., et al.: Buckling of a stiff thin film on a compliant substratein large deformation. Int. J. Solids Struct. **45**, 3107–3121 (2008)
55. Huang, R.: Kinetic wrinkling of an elastic film on a viscoelastic substrate. J. Mech. Phys. Solids **53**, 63–89 (2005)
56. Li, T., Suo, Z.: Ductility of thin metal films on polymer substrates modulated by interfacial adhesion. Int. J. Solids Struct. **44**, 1696–1705 (2007)
57. Baca, A.J., Ahn, J.H., Sun, Y., et al.: Semiconductor wires and ribbons for high-performance flexible electronics. Angew. Chem. Int. Ed. **47**, 5524–5542 (2008)
58. Song, J., Jiang, H., Huang, Y., et al.: Mechanics of stretchable inorganic electronic materials. J. Vac. Sci. Technol. A **27**, 1107–1125 (2009)
59. Timoshenko, S.P., Gere, J.M.: Theory of Elastic Stability. McGraw-Hill, New York (1963)
60. Song, J., Huang, Y., Xiao, J., et al.: Mechanics of non-coplanar mesh design for stretchable electronic circuits. J. Appl. Phys. **105**, 123516 (2009)
61. Wang, S., Xiao, J., Jung, I., et al.: Mechanics of hemispherical electronics. Appl. Phys. Lett. **95**, 181912 (2009)
62. Kim, D.H., Xiao, J., Song, J., et al.: Stretchable, curvilinear electronics based on inorganic materials. Adv. Mater. **22**, 2108–2124 (2010)
63. Mcdonald, J.C., Whitesides, G.M.: Poly (dimethylsiloxane) as a material for fabricating microfluidic devices. Acc. Chem. Res. **35**, 491–499 (2002)
64. Maltezos, G., Nortrup, R., Jeon, S., et al.: Tunable organic transistors that use microfluidic source and drain electrodes. Appl. Phys. Lett. **83**, 10 (2003)
65. Kim, H.J., Son, Ch., Ziaie, B.: A multiaxial stretchable interconnect using liquid-alloy-filled elastomeric microchannels. Appl. Phys. Lett. **92**, 011904 (2008)
66. So, J.H., Thelen, J., Qusba, A., et al.: Reversibly deformable and mechanically tunable fluidic antennas. Adv. Funct. Mater. **19**, 3632–3637 (2009)
67. Siegel, A.C., Tang, S.K.Y., Nijhuis, C.A., et al.: Cofabrication: a strategy for building multicomponent microsystems. Acc. Chem. Res. **43**, 518–528 (2010)
68. Jones, J., Lacour, S.P., Wagner, S., et al.: Stretchable wavy metal interconnects. J. Vac. Sci. Technol. A **22**, 1723–1725 (2004)
69. Li, T., Suo, Z., Lacour, S.P., et al.: Compliant thin film patterns of stiff materials as platforms for stretchable electronics. J. Mater. Res. **20**, 3274–3277 (2005)

70. Brosteaux, D., Axisa, F., Gonzalez, M., et al.: Design and fabrication of elastic interconnections for stretchable electronic circuits. IEEE Electron Devices Lett. **28**, 552–554 (2007)
71. Zoumpoulidisa, T., Barteka, M., de Graafb, P., et al.: High-aspect-ratio through-wafer parylene beams for stretchable silicon electronics. Sens. Actuators A **156**, 257–264 (2009)
72. Hsu, Y.Y., Gonzalez, M., Wolf, I.D.: In situ observations on deformation behavior and stretchinginduced failure of fine pitch stretchable interconnect. J. Mater. Res. **24**, 3573–3582 (2009)
73. Kim, H.J., Maleki, T., Wei, P., et al.: A biaxial stretchable interconnect with liquid-alloy-covered joints on elastomeric substrate. J. Microelectromech. Syst. **18**, 138–146 (2009)
74. Lin, K.L., Jain, K.: Design and fabrication of stretchable multilayer self-aligned interconnects for flexible electronics and large-area sensor arrays using excimer laser photoablation. IEEE Electron Devices Lett. **30**, 14–17 (2009)
75. Ahn, J.H., Zhu, Z., Park, S.I., et al.: Defect tolerance and nanomechanics in transistors that use semiconductor nanomaterials and ultrathin dielectrics. Adv. Funct. Mater. **18**, 2535–2540 (2008)
76. Park, S.I., Ahn, J.H., Feng, X., et al.: Theoretical and experimental studies of bending of inorganic electronic materials on plastic substrates. Adv. Funct. Mater. **18**, 2673–2684 (2008)
77. Jiang, Z., Huang, Y., Chandra, A.: Thermal stresses in layered electronic assemblies. J. Electron. Packag. **119**, 127–132 (1997)
78. Wang, K.P., Huang, Y.Y., Chandra, A., et al.: Interfacial shear stress, peeling stress, and die cracking stress in trilayer electronic assemblies. IEEE TCPT **23**, 309–316 (2000)